10. S. G. Han, Z. V. Vardeny, K. S. Wong, O. G. Symko, G. Koren, *Phys. Rev. Lett.* **65**, 2708 (1990).
11. C. J. Stevens *et al.*, *Phys. Rev. Lett.* **78**, 2212 (1997) and references therein.
12. J. L. W. Siders, R. N. Jacobs, C. W. Siders, S. A. Trugman, S. A. Taylor, in *Ultrafast Phenomena XI*, T. Elsaesser *et al.*, Eds. (Springer, Berlin, 1998), pp. 365–367.
13. R. A. Kaindl, F. Eickemeyer, M. Woerner, T. Elsaesser, *Appl. Phys. Lett.* **75**, 1060 (1999).
14. H. F. Sakeek *et al.*, *J. Appl. Phys.* **70**, 2455 (1991).
15. G. A. Farnan, M. P. McCurry, D. G. Walmsley, unpublished data.
16. The excitation density in the experiments estimated from the average pump power (about 15 mW) and focus diameter (about 170 μm) was 1.5×10^{19} cm^{-3}.
17. S. D. Brorson *et al.*, *Phys. Rev. Lett.* **64**, 2172 (1990).
18. S. Yamaguchi and H. Hamaguchi, *J. Mol. Struct.* **379**, 87 (1996).
19. This interpretation of the results is supported by measurements with different excitation intensities, showing a different saturation behavior of the two components.
20. V. J. Emery, S. A. Kivelson, O. Tzachar, *Phys. Rev.* B **56**, 6120 (1997).
21. D. Pines, *Z. Phys. B* **103**, 129 (1997).
22. J. P. Carbotte, E. Schachinger, D. N. Basov, *Nature* **401**, 354 (1999).
23. D. Munzar, C. Bernhard, M. Cardona, *Phys.* C **312**, 121 (1999).
24. E. Demler and S.-C. Zhang, *Nature* **396**, 733 (1998).
25. Supported by the European Union through the Training and Mobility of Researchers Ultrafast Network. We thank C. Stevens, P. Hamm, C. Lienau, G. A. Wagner, and J. E. Evetts for discussions and contributions to early stages of this work.

3 September 1999; accepted 23 November 1999

All-Optical Magnetic Resonance in Semiconductors

J. M. Kikkawa and D. D. Awschalom*

A scheme is proposed wherein nuclear magnetic resonance (NMR) can be induced and monitored using only optical fields. In analogy to radio-frequency fields used in traditional NMR, circularly polarized light creates electron spins in semiconductors whose hyperfine coupling could tip nuclear moments. Time-resolved Faraday rotation experiments were performed in which the frequency of electron Larmor precession was used as a magnetometer of local magnetic fields experienced by electrons in n-type gallium arsenide. Electron spin excitation by a periodic optical pulse train appears not only to prepare a hyperpolarized nuclear moment but also to destroy it resonantly at magnetic fields proportional to the pulse frequency. This resonant behavior is in many ways supportive of a simple model of optically induced NMR, but a curious discrepancy between one of the observed frequencies and classic NMR values suggests that this phenomenon is more complex.

Hyperfine interactions have been invaluable in probing solid-state systems. Optical pumping and detection of NMR (*1–3*) are sensitive measures of localized electronic states in semiconductors (*4, 5*), and have advanced our understanding of spin polarization in the quantum Hall regime (*6*). Instabilities of the electron-nuclear system that manifest in hysteresis of the electron magnetization have long been recognized (*2, 7*), and in quantum Hall systems this interplay has recently been found to be strong enough to dominate charge transport characteristics (*8*). Electron-nuclear coupling may also allow for the manipulation of coherent nuclear states in quantum computation (*9*). Here we propose that such interactions may enable the manipulation and detection of nuclear spin states with entirely optical methods, a scheme relevant to a broad variety of materials systems in which electron spins can be optically oriented and exhibit hyperfine coupling to nuclei.

We have performed a series of experiments that reveal magnetic resonance phenomena in gallium arsenide (GaAs) semiconductors occurring in the vicinity of nuclear frequencies and induced by an optical pulse train. Using optical detection of the electron Larmor frequency as a sensitive magnetometer, we find that optical pumping induces local fields up to ~0.4 T in ~250 s, which is nine orders of magnitude slower than typical electronic time scales and is suggestive of nuclear polarization by conduction electrons. Furthermore, we propose that optical fields can resonantly tip nuclear moments, using periodically excited electron spin instead of conventional radio-frequency (RF) fields. Extending the technique of Larmor magnetometry, we discover a depolarization of local magnetic fields that is indeed resonant with the periodicity of optical excitation. One of the two observed resonances fields lies within measurement error of that predicted by our model for optical NMR, whereas the other differs by ~11% with the nearest isotope of the GaAs host. The latter finding is particularly surprising because the temperature and field dependence, time scale, linewidth, and optical saturation of the resonance amplitude are all consistent with our framework for NMR. Despite attempts to identify additional periodicities that might influence resonance, further study is necessary to clarify its underlying mechanism.

Time-resolved magneto-optical Faraday rotation, recently developed for measuring conduction band spin precession in semiconductors (*10–13*), is well suited for the study of nuclear moments in GaAs because the hyperfine interaction is particularly large in this semiconductor (*2*). Our pump-probe experiments use short (~100 fs) time-delayed optical pulses tuned near the band-gap energy of the semiconductor and focused to a diameter of ~20 μm. A circularly polarized pump pulse, incident along the sample normal $\hat{x}$, excites an electronic magnetization, $\vec{S} \| \hat{x}$. An in-plane external field, $\vec{B} \| \hat{z}$, induces the subsequent Larmor precession of $\vec{S}$ about $\hat{z}$. The projection of this spin motion along $\hat{x}$ is recorded by the Faraday rotation, θ_F, of a linearly polarized, time-delayed probe pulse ($\theta_F \propto S_x$). As the pump-probe delay Δt is scanned, precession of $\vec{S}(\Delta t)$ causes S_x (and thus θ_F) to oscillate at the Larmor frequency $\omega_L = g_e \mu_B B_{tot}/\hbar$. Because the total magnetic field B_{tot} is the sum of the applied field and any additional local fields experienced by the electrons, Larmor frequency measurements can be used for magnetometry of hyperfine fields whenever the electron g factor, g_e, is known to be constant.

Electron spin precession for an n-type GaAs crystal with $n = 3 \times 10^{16}$ cm^{-3} and a transverse field strength of $B = 5.19$ T is shown in Fig. 1A. The sample is held at temperature (T) = 5 K inside a magnetooptical cryostat containing a superconducting magnet. Details of sample preparation and measurement are given elsewhere (*12*). The pump's arrival at $\Delta t = 0$ initiates spin motion whose oscillatory frequency reflects a g factor of −0.44 and responds dynamically to changes in B_{tot}. The oscillation decay time T_2^*, despite a 100-fold decrease relative to data taken in zero field (*12*), exceeds the Larmor period by roughly two orders of magnitude and allows ω_L to be determined to high precision. Successive measures of ω_L can then be used to capture changes in B_{tot} over long time scales.

Because nuclear polarization can shift the electron spin resonance line (*14*), nuclear dynamics induced by optical pumping should be measureable in real-time measurements of the Larmor frequency. Instead of studying ω_L by capturing dozens of spin revolutions, as in Fig. 1A, we monitored a single revolution near the end of such a scan and used shifts in the Larmor angle, $\omega_L \Delta t$, to establish changes in ω_L at a fixed value of the applied field. This strategy improved temporal resolution, and by repeatedly sweeping Δt from 2660 to 2700 ps, the dynamics of $B_{tot} \propto \omega_L$ could be studied in 10-s intervals. The plot atop Fig. 1C shows the first scan, and subsequent scans are assembled in the

Department of Physics, University of California, Santa Barbara, CA 93106, USA.

*To whom correspondence should be addressed. E-mail: awsch@physics.ucsb.edu

grayscale image below. The sample was translated twice during measurement by ~1.5 mm to reveal optically pumped contributions to B_{tot}. This procedure exposed new areas to optical pumping, causing the disappearance and subsequent recovery of optically induced fields. The resulting discontinuities of the Larmor angle appeared as sudden changes in the spin precession phase (Fig. 1C, grayscale image). Scans of Δt taken from −300 to 2700 ps as in Fig. 1A (not shown in figure) reveal that these discontinuous shifts accompanied uniform expansions of the spin profile in time that arose from a decrease in ω_L and thus B_{tot}. This field change, ΔB_{tot}, is plotted against laboratory time in Fig. 1B and can be expressed as $\Delta B_{tot} \sim -B_{ind} \exp(-t/T_1)$, where $T_1 \sim 250$ s and B_{ind} characterizes the strength of the optically induced field. T_1 exceeds typical electronic times by at least nine orders of magnitude and is typical of nuclear optical pumping times in GaAs (*2*). Although B_{ind} is quite large in this case (0.12 T), it actually corresponds to only ~2% of the maximum hyperfine field available when spin 3/2 Ga^{69}, Ga^{71}, and As^{75} nuclei are fully polarized (*5*).

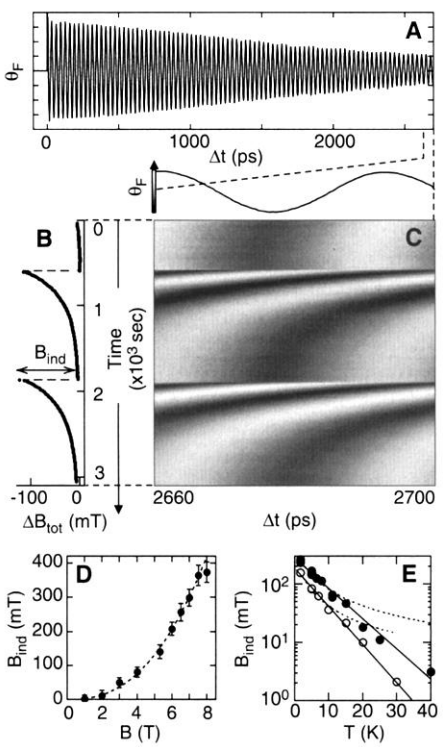

Fig. 1. (**A**) Time-resolved Faraday rotation θ_F in $n = 3 \times 10^{16}$ cm^{-3} GaAs at $B = 5.19$ T. (**B**) Relative magnetic field changes ΔB_{tot} versus laboratory time. The sample was translated at 600 and 1860 s. (**C**) Faraday rotation data used to extract ΔB_{tot}. A horizontal cut through the grayscale image represents an individual scan of θ_F versus Δt, as shown atop (C), where raw data at time = 0 is plotted with a vertical axis that encodes the grayscale information. (A) through (C) were taken at $T = 5$ K, a photon energy $E_\gamma = 1.50$ eV, and a total pump pulse energy $E_P = 13$ μJ cm^{-2}. (**D**) The optically induced field versus magnetic field at $T = 5$ K. The dotted line indicates a fit to $B_{ind} \sim B^{5/2}$. Error bars indicate 90% confidence intervals. (**E**) The temperature dependence of B_{ind} at $B = 5.19$ T on a log scale for two excitation powers. (D) and (E) were taken at $E_\gamma = 1.51$ eV and $E_P = 13$ μJ cm^{-2}, except in (E) where the open circles were taken at $E_P = 1.9$ μJ cm^{-2}. Each point in (D) and (E) was obtained by sample translation after a 30-min saturation interval.

Optical pumping can orient nominally unpolarized nuclei in this experiment, because the pump introduces nonequilibrium electron spins that attempt to thermally equilibrate, in part by flipping nuclear spins. This process of nuclear hyperpolarization is known as the Overhauser effect (*1, 2, 15*) and is governed by the deviation of the electron spin polarization from its thermal equilibrium value. Because the time scale for the Overhauser process is orders of magnitude slower than the electron Larmor frequency, the nuclear system sees an optically excited electronic system that is largely depolarized by spin precession. Time-averaging the $\hat{x}$ and $\hat{y}$ electron spin components gives

$$\bar{S}_x = S_0 \frac{(\omega_L T_2^*)(T_2^*/t_{rep})}{1 + (\omega_L T_2^*)^2} \approx \frac{S_0}{\omega_L t_{rep}} \quad (1)$$

and $\bar{S}_y = (\omega_L T_2^*)\bar{S}_x$ where S_0 is the electron spin excited by each pulse and $\omega_L T_2^* \gg 1$. Because the pump arises from the periodic output of a Ti:sapphire laser (~76 MHz), its repetition interval t_{rep} has been included (*12*). Precession depolarizes the time-averaged transverse spin component $\bar{S}_\perp = (\bar{S}_x^2 + \bar{S}_y^2)^{1/2}$ by a factor $\bar{S}_\perp/S_0 \approx 10^{-4}$ to 10^{-3} for fields above 1 T. This effect gives rise to an increased effective spin temperature, T_{eff}, for the nominally paramagnetic electron spins. As electrons attempt to repolarize, the Overhauser process results in a nuclear-level population, $N(I_z)/N(I_z - 1) = e^{g_e \mu_B B/k_B T_N}$, where $T_N \equiv (T^{-1} - T_{eff}^{-1})^{-1}$, I_z is the longitudinal nuclear spin, and k_B is Boltzmann's constant (*16*). Hence, the average polarization for nuclei in the GaAs matrix is given by the spin-3/2 Brillouin function $Br_{3/2}$

$$\langle I_z \rangle = (3/2) f Br_{3/2}\left(\frac{3}{2}\frac{g_e \mu_B B}{k_B T_N}\right) \quad (2)$$

and is up to ~10^3 times larger than its nominal value as it is now determined by the electron Zeeman energy, not the nuclear Zeeman energy. The "leakage factor" f accounts for additional modes of spin relaxation (*2*).

Measurement of the induced field versus the applied field at 5 K shows qualitative deviations from the expected behavior (Eq. 2). Figure 1D shows a superlinear field dependence that cannot be fit with Eq. 2 for any value of T_N, as the Brillouin function is always sublinear in B. Figure 1E shows that the temperature dependence of B_{ind} at a field of 5.19 T seems to obey $B_{ind} \sim \exp(-\alpha T)$ (solid lines) rather than a best fit to Eq. 2 (dotted lines). Reducing the excitation power yielded no better agreement with Eq. 2 (open circles). To accurately account for the observed behavior within the framework of nuclear polarization, a formulation of the Overhauser process that explicitly includes transverse electron spin magnetization may be necessary. Additionally, it may be necessary to consider the coupling of nuclei to localized electronic states whose orbital character and occupancy may change with field and temperature.

If the optically induced moment is indeed of nuclear origin, one might expect that periodic excitation of electron spin with a small transverse component $\bar{S}_\perp$, given by Eq. 1, could tip this moment away from the applied field through the hyperfine interaction. Fully polarized, delocalized conduction electrons in GaAs exert a field on the order of 5.3 T × $(\mu_B n/\mu_N N)$ on the nuclei (*2*), where μ_N is the nuclear magneton and n and N are the electron and nuclear densities, respectively. This formula predicts a (Knight) shift of the NMR field that is in good agreement with experiment (*2, 6*), on the order of ~1 × 10^{-3} T at $n = 3 \times 10^{16}$ cm^{-3}. Hence, the spin polarization of Eq. 1 gives an average tipping field H_1 of ~10^{-6} T and a Rabi frequency of ~10 Hz for realistic pump-induced electron densities of 3 × 10^{17} cm^{-3} per pulse. This average field is periodic at the laser repetition frequency t_{rep}^{-1} and may be tuned into resonance with the nuclear Larmor frequency by adjusting t_{rep} and/or B. Tipping of nuclei then proceeds as in conventional NMR, but with the rotation of an existing nuclear moment occurring via optical fields. This process is fundamentally different than in low-field experiments, where the excited spin orientation is modulated in concert with the Larmor precession of nuclear moments (*2, 17*). Such experiments sustain an Overhauser enhancement within the nuclear rotating frame, generating transverse nuclear magnetization by thermodynamic cooling of the nuclear spins from an unpolarized initial state. In contrast, the resonance effects described here are only expected at higher magnetic fields and low temperatures, where optically pumped nuclear polarization is nonzero (Fig. 1, D and E).

By exciting the system at a fixed pump frequency and sweeping the applied magnetic field through the region of anticipated nuclear resonances, one might expect the above optical resonance phenomenon to modify the nuclear contribution to B_{tot} whenever a resonance condition is met. This measurement strategy was used to obtain the data in Fig. 2B, where real-time Larmor magnetometry monitored changes in B_{tot} for the $n = 3 \times 10^{16}$ cm^{-3} sample while sweeping B from 5.21 to 5.43 T. The presentation is similar to that in Fig. 1C, except that the applied magnetic field increased linearly along with laboratory time on the vertical axis, as indicated. Although B_{tot} is nominally expected to increase nearly linearly with B (with super-

linear contributions coming from the Overhauser polarization, as in Fig. 1D), its actual evolution was dramatically different. As shown in Fig. 2A, B_{tot} increased linearly but suddenly decreased at $B = 5.256$ T. Its subsequent recovery was given by the same exponential that characterized optical pumping of local fields after sample displacement, suggesting that the anomalous changes in B_{tot} seen in Fig. 2A arose from a depolarization of the optically induced field.

A resonant relation between the field at which depolarization occurred, B_1, and the pump pulse frequency was established by elongating the laser cavity and thereby decreasing the pump repetition rate from a nominal 76 MHz. A simple proportionality $\nu_{pump} = t_{rep}^{-1}$ was seen between B_1 and the pulse frequency (0.0692 ± 0.0010 T/MHz) (Fig. 2C). Moreover, a second discontinuity appeared at $B_2 = (1.428 \pm 0.001)^* B_1 = 0.0988 \pm 0.0015$ T/MHz. Both resonance fields remained at these same values for a lower doped, $n = 1 \times 10^{16}$ cm^{-3} sample, and were not observed in the two higher doping concentrations studied ($n = 2 \times 10^{17}$ or $n = 3 \times 10^{17}$ cm^{-3}).

The above data reveal a magnetic resonance phenomenon that is induced by the optical field. B_2 lies within measurement error of the standard NMR field for Ga^{69} (0.097852 T/MHz), in agreement with a scenario of optically induced NMR. B_1, in contrast, shows surprising deviations from any likely candidates for nuclear resonance in this system, which include the two remaining spin-3/2 isotopes within the GaAs matrix (Ga^{71} and As^{75}) and the spin-1/2 Si^{29} donors. We dismiss any association with the latter because we observe similar behavior in modulation-doped GaAs/AlGaAs quantum wells ($n \sim 4 \times 10^{11}$ cm^{-2}), where there is no Si in contact with the two-dimensional electron gas (2DEG) (*18*). Of these isotopes, the resonance field for Ga^{71} (0.077021 T/MHz) lies closest to B_1 and yet still differs by ~11%. Because the applied magnetic field was monitored by a cryogenic Hall sensor, commercially calibrated to 0.5% accuracy, and these measurements were repeated in a second magnetooptical cryostat to verify reproducibility of field calibrations, we believe this discrepancy lies well beyond our measurement error.

These findings are unusual because traditional NMR for these nuclear species has been reported close to standard values in a variety of doped GaAs heterostructures, thin films, and bulk crystals (*3, 5–8, 17*), even when selectively probing nuclei in the strong fields of localized electrons (*7*). Knight shifts in these systems are typically no more than 0.01% at comparable fields (*2, 6*). Anomalous hyperfine splittings of Ga NMR lines have been recently measured in Ga nuclei coupled to a 2DEG (*19*), and are also only a 0.01% effect. Quadrupolar effects can dominate in GaAs with substitutional impurities, but these are small at high fields and depend on crystal orientation (*2, 20*). In contrast, we found that tilting the [100] axis ± 25° from the pump direction had no measurable effect on B_1 or B_2.

To explore the possibility that our basic model for NMR via hyperfine fields ignores additional factors that determine resonance, we systematically varied other periodicities within the experiment. A 50-kHz polarization modulation on the pump beam was generally used to increase the signal-to-noise ratio, but this does not appear to affect the resonance positions as these were unchanged when using a statically polarized pump. Additional periodicities arise from pump-probe temporal separations at $nt_{rep} \pm \Delta t$, and to study their effect we illuminated the sample with an additional pump P_2 while simultaneously using the original pump-probe pair for Larmor magnetometry. Detuning P_2's pulse train frequency from the original pump P rendered its arrival incoherent with respect to the probe, and yet the associated resonance field shift was the same as in Fig. 2C. Hence, the observed resonance fields seem unrelated to the pump-probe interval. Thus, the discrepancy of B_1 with standard resonance values remains unresolved and suggests that our proposal for optically induced nuclear resonance, in which the Larmor precession of electron spins has been averaged away, may be oversimplified.

The dual pump configuration used above allowed us to determine the line width of this new optical resonance. An acoustooptic modulator shuttered P_2, while local field changes were recorded by the original pump-probe pair. Depolarization responses to P_2 were studied versus P_2's pulse frequency in a static external field that was far off resonance from the original pump (Fig. 3A). The corresponding T_2^* time for the B_1 resonance was $\sim 10^{-4}$ s, in good agreement with nuclear transverse spin times in GaAs (*2, 6*).

Within our model for optically induced NMR, transverse nuclear magnetization can be either maintained or destroyed during the tipping process, depending on the strength of the hyperfine field. The former "coherent" rotation is possible when the tipping field $H_1 \geq (T_2^{*N}\gamma)^{-1}$, where $\gamma \equiv g_N\mu_N/\hbar$ is the nuclear gyromagnetic ratio and T_2^{*N} is the inhomogeneous nuclear transverse spin lifetime. For smaller H_1, transverse nuclear magnetization decays between tipping pulses and gives rise to an exponential depolarization of the longitudinal nuclear spin at a rate $(\gamma H_1)^2 T_2^{*N}$ (*1, 16*). Because $T_2^{*N} \sim 10^{-4}$ s and γ is of order $2\pi \times 10^7$ rad-s^{-1} T^{-1} in GaAs, we expect delocalized electrons to contribute primarily to the latter "incoherent depolarization" in a time ~1 s. Fully polarized, localized electrons may exert fields of 100 to 200 G (*5*) and can give rise to the former "coherent" tipping phenomena. Our data appear to be most consistent with an incoherent process. Figure 3B shows depolarization measured against P_2 exposure time, along with a fit to an exponential saturation with a time $\tau \sim 0.9$ s that agrees with our above estimate of the NMR tipping field due to delocalized electrons. One might also consider that only nuclei near localized electrons are directly tipped by electrons and that depolarization proceeds via nuclear spin diffusion. This scenario appears unlikely, however, because depolarization would be expected to saturate in a much slower time of $a^2/D_N \sim 100$ s, where $a \sim n^{-1/3}$ is the mean distance between localized electrons and $D_N \sim 10^{-13}$ cm^2 s^{-1} is the nuclear spin diffusion constant (*5, 21*).

In either tipping process, one expects that depolarization will be proportional to the initial size of the induced moment. Resonant depolarization at B_1 indeed scaled with temperature-dependent changes in B_{ind} (characterized near B_1) (Fig. 3C). Here, resonant depolarization is

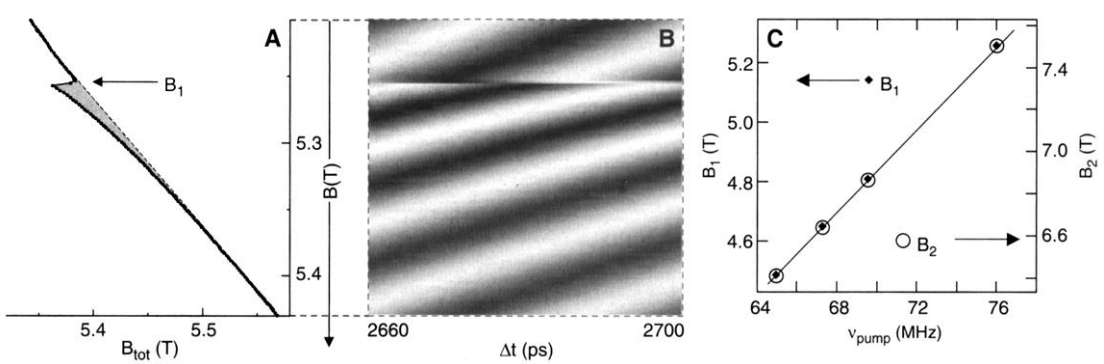

Fig. 2. (**A**) B_{tot} measured as B is increased from 5.21 to 5.43 T at 0.01 T min^{-1}. (**B**) Faraday rotation used to produce (A), depicted in the same manner as in Fig. 1C, except that B increases along the laboratory time axis. Note the spontaneous discontinuity at $B = B_1$. (**C**) Resonance fields B_1 and B_2 versus pump frequency. Data were taken with $n = 3 \times 10^{16}$ cm^{-3} at $T = 5$ K, $E_\gamma = 1.50$ eV for (A) and (B) and 1.51 eV for (C), and $E_p = 13$ μJ cm^{-2}.

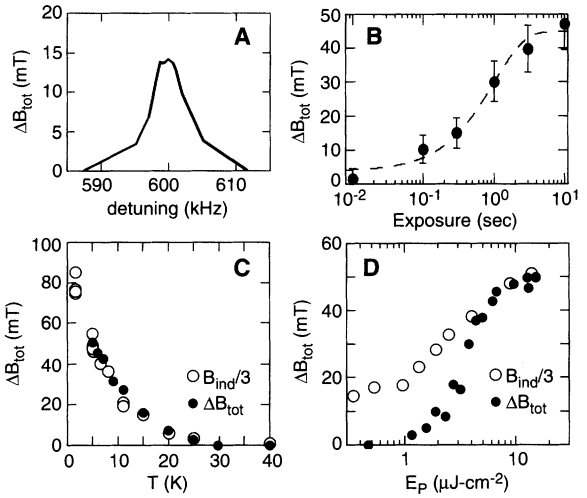

Fig. 3. Relative changes ΔB_{tot} induced by exposure to an additional, statically polarized pump beam, P_2, as a function of (**A**) P_2's detuning at an exposure of 0.3 s and (**B**) P_2's exposure at a detuning of +600.0 kHz. B_{tot} was saturated for 30 min under P illumination before data collection at T = 5 K and B = 5.297 T. The dotted fit in (B) is described in the text. Error bars indicate 90% confidence intervals. (**C**) A comparison of optically induced local fields near B_1 (open circles) and resonant depolarization shifts at B_1 (solid circles) for 1.6 K < T < 40 K. The former were taken from Fig. 1E and scaled by 1/3, and the latter were measured by sweeping B through B_1, as in Fig. 2, (A) and (B), with dB/dt = 0.001 T min^{-1}. (**D**) Same data taken at T = 5 K for various E_p. All data were taken with E_γ = 1.51 eV and E_p = 13 μJ cm^{-2}. In (C) and (D) a single pump laser was used, and in (A) and (B) P_2's energy was 7 μJ cm^{-2}.

obtained using the method of Fig. 2. However, these resonant shifts fail to scale with B_{ind} as the excitation density changes at T = 5 K (Fig. 3D). Such behavior is consistent with optically induced NMR because the tipping field itself is expected to be proportional to the excitation density.

The observed magnetic resonance behavior is both qualitatively and in some ways quantitatively consistent with a scenario of incoherent nuclear depolarization by delocalized electrons. The lower resonance field exhibits a perplexing departure from that expected for any nuclei in the host semiconductor, suggesting that the simple picture of resonance presented here is incomplete. Although one should consider alternative explanations, it is nevertheless difficult to image that B_1 (or B_2) is associated with an electronic moment. Comparably long electronic T_1 times have only been observed for donor localized electrons in silicon (*4*), and in that case depended sensitively on carrier density, donor concentration, and temperature. In contrast, the resonances we observe are somewhat immune to changes in the electronic environment and occur at the same values independent of not only the above parameters but also the excitation density. A hybrid experiment integrating both traditional NMR and this new optical resonance technique may help to clarify the relationship between these two phenomena. Ultimately, we believe that all-optical NMR may combine with local optical probes to address individual donor states whose tipping fields can be considerably stronger. Such a strategy might then enable coherent manipulation of individual nuclear spins, a first step in establishing optical control over solid-state nuclear spin coherence.

Note added in proof: Recent studies in quantum structures indicate that B_1 may be related to a harmonic of the As resonance (*18*).

References and Notes

1. C. P. Slichter, *Principles of Magnetic Resonance* (Springer-Verlag, New York, ed. 2, 1978).
2. *Optical Orientation*, F. Meier and B. P. Zakharchenya, Eds. (North-Holland, New York, 1984).
3. J. A. Marohn *et al.*, *Phys. Rev. Lett.* **75**, 1364 (1995).
4. G. Feher, *Phys. Rev.* **114**, 1219 (1959); G. Feher and E. A. Gere, *Phys. Rev.* **114**, 1245 (1959).
5. D. Paget, G. Lampel, B. Sapoval, V. I. Safarov, *Phys. Rev. B* **15**, 5780 (1977); D. Paget, *Phys. Rev. B* **24**, 3776 (1981); *Phys. Rev. B* **25**, 4444 (1982).
6. R. Tycko, S. E. Barrett, G. Dabbagh, L. N. Pfeiffer, K. W. West, *Science* **268**, 1460 (1995); N. N. Kuzma, P. Khandelwal, S. E. Barrett, L. N. Pfeiffer, K. W. West, *Science* **281**, 686 (1998).
7. M. Seck, M. Potemski, P. Wyder, *Phys. Rev. B* **56**, 7422 (1997).
8. D. C. Dixon, K. R. Wald, P. L. McEuen, M. R. Melloch, *Phys. Rev. B* **56**, 4743 (1997); H. Cho *et al.*, *Phys. Rev. Lett.* **81**, 2522 (1998); S. Kronmuller *et al.*, *Phys. Rev. Lett.* **81**, 2526 (1998).
9. B. E. Kane, *Nature* **393**, 133 (1998).
10. S. A. Crooker, J. J. Baumberg, F. Flack, N. Samarth, D. D. Awschalom, *Phys. Rev. Lett.* **77**, 2814 (1996).
11. J. M. Kikkawa, I. P. Smorchkova, N. Samarth, D. D. Awschalom, *Science* **277**, 1284 (1997).
12. J. M. Kikkawa and D. D. Awschalom, *Phys. Rev. Lett.* **80**, 4313 (1998).
13. J. M. Kikkawa and D. D. Awschalom, *Phys. Today* **52**, 33 (1999) and references therein.
14. V. L. Berkovitz, C. Hermann, G. Lampel, A. Nakamura, V. I. Safarov, *Phys. Rev. B* **18**, 1767 (1978).
15. A. W. Overhauser, *Phys. Rev.* **92**, 411 (1953); A. Abragam, *Phys. Rev.* **98**, 1729 (1955).
16. A. Abragam, *The Principles of Nuclear Magnetism* (Clarendon Press, Oxford, 1961).
17. V. P. Zakharchenya, M. E. Kompan, V. G. Fleisher, *Zh. ETF Pis. Red.* **19**, 734 (1974) [*J. Exp. Theor. Phys. Lett.* **19**, 378 (1974)].
18. G. Salis *et al.*, unpublished data.
19. S. Kronmuller *et al.*, *Phys. Rev. Lett.* **82**, 4070 (1999).
20. V. A. Novikov, V. G. Fleisher, *Zh. Eksp. Teor. Fiz.* **74**, 1026 (1978) [*Sov. Phys. J. Exp. Theor. Phys.* **47**, 539 (1978)].
21. V. K. Kalevich *et al.*, *Pis'ma Zh. Eksp. Teor. Fiz.* **35**, 17 (1982) [*J. Exp. Theor. Phys. Lett.* **35**, 20 (1982)].

22. Supported by grant DAAG55-98-1-0366 from the Army Research Office, by grant N00014-99-1096 from DARPA/ONR, and by grants DMR-9701072 and QUEST STC DMR-91-20007 from NSF.

30 July 1999; accepted 29 November 1999

Trienoic Fatty Acids and Plant Tolerance of High Temperature

Yuuki Murakami,[1] Michito Tsuyama,[2] Yoshichika Kobayashi,[2] Hiroaki Kodama,[1]* Koh Iba[1]†

The chloroplast membrane of higher plants contains an unusually high concentration of trienoic fatty acids. Plants grown in colder temperatures have a higher content of trienoic fatty acids. Transgenic tobacco plants in which the gene encoding chloroplast omega-3 fatty acid desaturase, which synthesizes trienoic fatty acids, was silenced contained a lower level of trienoic fatty acids than wild-type plants and were better able to acclimate to higher temperatures.

In some desert and evergreen plants, an increase in the growth temperature leads to a reduction in trienoic fatty acids α-linolenic acid (18:3) and hexadecatrienoic acid (16:3) (*1*, *2*). In order to investigate the physiological effect of these fatty acids in plants grown at high temperatures, we constructed transgenic tobacco plants in which the expression of the chloroplast trienoic fatty acid synthetase gene was inhibited.

Transgenic tobacco plants harboring transferred DNA (T-DNA) with the chloroplast-localized ω-3 desaturase gene (*FAD7*) from *Arabidopsis thaliana* under the control of the cauliflower mosaic virus 35*S* promoter were generated (*3*). Gene-silencing and reduction of trienoic–fatty acid content were observed in four transgenic lines (*4*). Of the four lines, two lines (T15 and T23) exhibited a 3 : 1 segregation ratio of kanamycin resistance versus nonresistance in the next generation, suggesting that the T-DNA was inserted in one position in the genome. The T15 line was backcrossed twice to

[1]Department of Biology and [2]Department of Forestry, Kyushu University, Fukuoka 812-8581, Japan.

*Present address: Department of Bioresources Chemistry, Faculty of Horticulture, Chiba University, Matsudo 648, Chiba 271-8510, Japan.

†To whom correspondence should be addressed. E-mail: koibascb@mbox.nc.kyushu-u.ac.jp